

## Structural Engineering of Porphyrin-based Small Molecules as Donors for Efficient Organic Solar Cells

Hongda Wang, Liangang Xiao, Lei Yan, Song Chen, Xunjin Zhu, Xiaobin Peng, Xingzhu Wang, Wai-Kwok Wong, Wai-Yeung Wong

### 1. Experimental section

**Conventional Device fabrication.** Solution-processed BHJ OSCs were fabricated as follows: Indium tin oxide (ITO) coated glass substrates were cleaned prior to device fabrication by sonication in acetone, detergent, distilled water, and isopropyl alcohol. After treated with an oxygen plasma for 5 min, 40 nm thick poly(styrene sulfonate)-doped poly(ethylene-dioxythiophene) (PEDOT:PSS) (Bayer Baytron 4083) layer was spin-coated on the ITO-coated glass substrates at 2500 rpm for 30s, the substrates were subsequently dried at 140°C for 20 min in air and then transferred to a N<sub>2</sub>-glovebox. The active layers were spun from chlorobenzene solution of donor/PC<sub>71</sub>BM at weight ratio of 1:0.5, 1:1, 1:2 and 1:3 with an overall concentration of 20 mg/mL. The thicknesses of active layers were measured by a profilometer. The active layer was annealed at different temperatures and time on hotplate in glovebox. The ultra-thin PFN layer was deposited by spin casting from a 0.02% (w/v) solution in methanol (from 2000 rpm for 30 s). Finally, Al (~80 nm) was evaporated with a shadow mask as the top electrode. The effective area was measured to be 0.16 cm<sup>2</sup>.

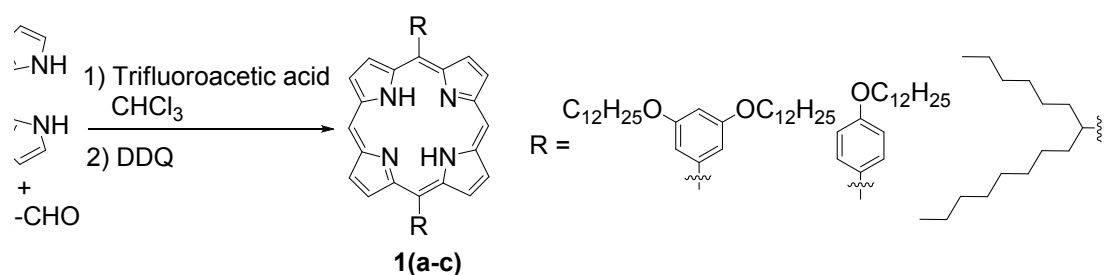
**Inverted Device fabrication.** The inverted photovoltaic devices were processed and characterized in ambient atmosphere. Indium tin oxide (ITO) coated glass substrates were cleaned prior to device fabrication by sonication in acetone, detergent, distilled water, and isopropyl alcohol. After treated with an oxygen plasma for 5 min, the ZnO electron transport/hole blocking layer was prepared by spin-coating at 5000 rpm from a

ZnO precursor solution prepared from 0.5 M zinc acetate dehydrate in 0.5 M monoethanolamine and 2-methoxyethanol under N<sub>2</sub>. After cleaning the electrical contacts, substrates were immediately baked in air for 5 min. The films were then rinsed with DI water, isopropanol, and acetone, and then dried in a glovebox. Active layer solutions was prepared from the solution of SM:PC<sub>71</sub>BM (1:1.2 weight ratio) in chlorobenzene (SM concentration: 15 mg/mL). For optimum performance devices, active layers was spin-coated 1000 rpm to obtain thicknesses of ~100 nm. Finally 10 nm MoO<sub>3</sub> and 100 nm Ag were deposited sequentially under  $6 \times 10^{-6}$  Torr by thermal evaporation through a shadow mask to form an active area of 0.16 cm<sup>2</sup>.

**Atomic force microscopy:** The atomic force microscopy (AFM) measurements of the surface morphology of blend films were conducted on a NanoScope NS3A system (Digital Instrument). The *J-V* characteristics were measured under AM 1.5 solar simulator (Japan, SAN-EI, XES-40S1) at 100 mW cm<sup>-2</sup>, and data was collected using a Keithley 2400 digital source meter. The spectral response was measured with a DSR100UV-B spectrometer with a SR830 lock-in amplifier. A calibrated Si photodiode was used as a reference before each measurement.

**Characterization.** <sup>1</sup>H NMR spectra were recorded using a Bruker Ultrashield 400 Plus NMR spectrometer. UV-vis spectra of dilute solutions ( $1 \times 10^{-5}$  M) of samples in dichloromethane were recorded at room temperature (*ca.* 25°C) using a Varian Cary 100 UV-vis spectrophotometer. Solid films for UV-vis spectroscopic analysis were obtained by spin-coating the molecule solutions onto a quartz substrate. Cyclic voltammetry (CV) of the molecule films was performed using a Versastat II electrochemical workstation operated at a scan rate of 50 mV s<sup>-1</sup>; the solvent was anhydrous MeCN, containing 0.1 M tetrabutylammonium hexafluorophosphate (TBAPF<sub>6</sub>) as the supporting electrolyte. The potentials were measured against a Ag/Ag<sup>+</sup> (0.01 M AgNO<sub>3</sub>) reference electrode; the ferrocene/ferrocenium ion (Fc/Fc<sup>+</sup>)

pair was used as the internal standard (0.09 V). The onset potentials were determined from the intersection of two tangents drawn at the rising and background currents of the cyclic voltammograms. HOMO and LUMO energy levels were estimated relative to the energy level of the ferrocene reference (4.8 eV below vacuum level). High-resolution matrix-assisted laser desorption/ionization time-of-flight (MALDI-TOF) mass spectra were obtained with a Bruker Autoflex MALDI-TOF mass spectrometer. Topographic and phase images of the polymer: PC<sub>71</sub>BM films (surface area: 5 × 5 μm<sup>2</sup>) were obtained using a Digital Nanoscope III atomic force microscope operated in the tapping mode under ambient conditions. The thickness of the active layer of the device was measured using a Veeco Dektak 150 surface profiler. The *J-V* characteristics were measured under AM 1.5 solar simulator (Japan, SAN-EI, XES-40S1) at 100 mW cm<sup>-2</sup>, and data was collected using a Keithley 2400 digital source meter. The spectral response was measured with a DSR100UV-B spectrometer with a SR830 lock-in amplifier. A calibrated Si photodiode was used as a reference before each measurement. Ultraviolet photoelectron spectroscopy (UPS) measurements were conducted on a KRATOS Axis Ultra DLD spectrometer with a base pressure of 3 × 10<sup>-8</sup> Torr, and He I (21.22 eV) was applied as the excitation source.



**Scheme S1.** Synthetic route for 1(a-c).

## 2. Synthesis procedures

**General procedure for 1(a–c).** Aldehyde derivatives (1.71 mmol) and dipyrromethane (0.25 g, 1.71 mmol) were dissolved in 300 mL of fresh dry chloroform, and the solution was purged with dry argon for 15 min. Then trifluoroacetic acid (TFA) (107  $\mu$ L, 1.41 mmol) was added by syringe quickly and the solution was stirred in dark under argon atmosphere at room temperature for 3 h. After that, DDQ (500 mg, 2.21 mmol) was added and the solution was stirred for additional 30 min before quenched by triethylamine (TEA) (1.5 mL, 10.7 mmol). The solvent was evaporated and the black solid was eluted with chloroform through a short pad of silica gel to remove most of the tar. The crude product was further purified by flash column chromatography twice using hexane/DCM (2:1) as the eluent and recrystallized from methanol to give pure product as dark brown red solid.

**5,15-Bis(3,5-di(dodecyloxy)phenyl)porphyrin (1a).**  $^1\text{H}$  NMR (400 MHz,  $\text{CDCl}_3$ ,  $\delta$ ): -3.13 (s, 2H), 0.93 (m, 12H), 1.39 (m, 60H), 1.53 (m, 12H), 1.91 (m, 8H), 4.18 (t,  $J = 4.8\text{Hz}$ , 8H), 6.94 (s, 2H), 7.44 (d,  $J = 2.0\text{ Hz}$ , 4H), 9.21 (d,  $J = 4.4\text{ Hz}$ , 4H,  $\beta$ -pyrrolic H), 9.39 (d,  $J = 4.8\text{Hz}$ , 4H,  $\beta$ -pyrrolic H), 10.30 (s, 2H).

**5,15-Bis(4-dodecyloxyphenyl)porphyrin (1b).**  $^1\text{H}$  NMR (400 MHz,  $\text{CDCl}_3$ ,  $\delta$ ): -3.16 (s, 2H), 0.97 (t,  $J = 6.8\text{Hz}$ , 6H,  $\text{CH}_3$ ), 1.31–1.38 (m, 32H), 1.51–1.52 (m, 4H), 1.61–1.67 (m, 4H), 4.23–4.24 (m, 4H), 7.32 (d,  $J = 8.4\text{ Hz}$ , 4H), 8.17 (d,  $J = 8.0\text{ Hz}$ , 4H), 9.13 (d,  $J = 4.4\text{ Hz}$ , 4H,  $\beta$ -pyrrolic H), 9.37 (d,  $J = 4.8\text{Hz}$ , 4H,  $\beta$ -pyrrolic H), 10.28 (s, 2H).

**5,15-Bis(2-hexylnonyl)-porphyrin (1c).**  $^1\text{H}$  NMR (400 MHz,  $\text{CDCl}_3$ ,  $\delta$ ): -2.44 (s, 2H), 0.65–0.73 (m, 12H), 0.99–1.10 (m, 30H), 1.16–1.38 (m, 8H), 1.48–1.59 (m, 6H), 2.76 (m, 4H), 2.97 (m, 4H), 5.20 (m, 2H), 9.43 (m, 4H,  $\beta$ -pyrrolic H), 9.65 (m, 2H,  $\beta$ -pyrrolic H), 9.75 (m, 2H,  $\beta$ -pyrrolic H), 10.21 (m, 2H).

**General procedure for 2(a–c).** To a two-neck round flask N-bromosuccinimide (471 mg, 2.647 mmol) was added to compound **1(a–c)** (1.20 mmol) in 200 mL chloroform under nitrogen. The mixture was stirred at room temperature for 0.5 h, and quenched with 200 mL

of methanol. After the filtration, the solid was dissolved in 200 mL chloroform and 0.5 mL of pyridine, followed by the addition of  $\text{Zn}(\text{OAc})_2 \cdot 2\text{H}_2\text{O}$  (664 mg, 3 mmol) in methanol (10 mL). And the reaction mixture was stirred overnight at room temperature. The solvents were removed, and the residue was washed with ethanol three times and then purified by column chromatography using  $\text{CHCl}_3/\text{hexane}$  (3:1) as the eluent. A purple solid was obtained after the recrystallization from DCM/ethanol.

**(10,20-Bis(3,5-di(dodecyloxy)phenyl)-5,15-dibromo-porphyrinato)zinc(II) (2a).**  $^1\text{H}$  NMR (400 MHz,  $\text{CDCl}_3$ ,  $\delta$ ): 0.85 (m, 12H), 1.22 (m, 64H), 1.43 (m, 8H), 1.88 (m, 8H), 4.08 (t,  $J = 6.55$  Hz, 8H), 6.78 (s, 2H), 7.24 (s, 4H), 9.02 (d,  $J = 4.8$  Hz, 4H,  $\beta$ -pyrrolic H), 9.66 (d,  $J = 4.8$  Hz, 4H,  $\beta$ -pyrrolic H).

**(10,20-Bis(4-dodecyloxyphenyl)-5,15-dibromo-porphyrinato)zinc(II) (2b).**  $^1\text{H}$  NMR (400 MHz,  $\text{CDCl}_3$ ,  $\delta$ ): 0.94 (t, 6H), 1.32–1.65 (m, 36H), 2.04 (m, 4H), 4.28 (t,  $J = 4.0$  Hz, 4H), 7.29 (d,  $J = 8.4$  Hz, 4H), 8.05 (d,  $J = 8.4$  Hz, 4H), 8.97 (d,  $J = 4.8$  Hz, 4H,  $\beta$ -pyrrolic H), 9.70 (d,  $J = 4.8$  Hz, 4H,  $\beta$ -pyrrolic H).

**(10,20-Bis(2-hexylnonyl)-5,15-dibromoporphyrinato)zinc(II) (2c).**  $^1\text{H}$  NMR (400 MHz,  $\text{CDCl}_3$ ,  $\delta$ ): 0.70 (t,  $J = 6.8$  Hz, 12H), 0.88–0.99 (m, 30H), 1.01–1.25 (m, 8H), 1.40–1.47 (m, 6H), 2.60–2.65 (m, 4H), 2.76–2.85 (m, 4H), 5.06–5.11 (t, 2H), 9.58 (d,  $J = 4.0$  Hz, 2H,  $\beta$ -pyrrolic H), 9.63 (d,  $J = 5.6$  Hz, 2H,  $\beta$ -pyrrolic H), 9.65 (d,  $J = 3.2$  Hz, 4H,  $\beta$ -pyrrolic H).

**General procedure for 3(a-c).** A mixture of **2(a-c)** (0.137 mmol) and 4-ethynyl-2,5-bis(hexyloxy)benzaldehyde (90.9 mg, 0.275 mmol) in THF (10 mL) and  $\text{Et}_3\text{N}$  (3 mL) was degassed with nitrogen for 10 min, then  $\text{Pd}(\text{PPh}_3)_4$  (25 mg, 0.022 mmol),  $\text{CuI}$  (5 mg, 0.022 mmol) were added to the mixture, and the solution was refluxed for 12 h under nitrogen. The solvent was removed under vacuum, and the solid residue was purified by preparative thin layer chromatography using a  $\text{CHCl}_3/\text{hexane}$  (3:1) as eluent. Recrystallization from  $\text{CHCl}_3/\text{methanol}$  gave **3c** as a green solid.

**3a.** 232.5 mg, 78% yield.  $^1\text{H}$  NMR (400 MHz,  $\text{CDCl}_3$ ,  $\delta$ ): 0.74–0.89 (m, 24H,  $\text{CH}_3$ ), 1.15–1.42 (m, 92H,  $\text{CH}_2$ ), 1.61–1.73 (m, 8H), 1.79–1.87 (m, 8H), 2.08–2.13 (m, 4H), 3.88–3.91 (m, 4H), 4.07–4.11 (m, 8H), 4.16–4.20 (m, 4H), 6.86–6.87 (m, 2H), 7.08 (s, 2H), 7.31 (s, 2H), 7.33 (s, 4H), 8.94 (d,  $J = 4.4\text{Hz}$ , 2H,  $\beta$ -pyrrolic H), 9.66 (d,  $J = 4.8\text{Hz}$ , 4H,  $\beta$ -pyrrolic H), 10.16 (s, 2H, CHO).

**3b.** 174.0 mg, 79% yield.  $^1\text{H}$  NMR (400 MHz,  $\text{CDCl}_3$ ,  $\delta$ ): 0.78–0.87 (m, 18H,  $\text{CH}_3$ ), 1.18–1.37 (m, 60H,  $\text{CH}_2$ ), 1.43–1.52 (m, 4H,  $\text{CH}_2$ ), 1.58–1.64 (m, 4H), 1.85–2.01 (m, 4H), 3.41–3.44 (m, 4H), 3.85–3.88 (m, 4H), 4.20–4.23 (m, 4H), 6.35 (s, 2H), 6.92 (s, 2H), 7.24 (d,  $J = 8.4\text{Hz}$ , 4H), 8.03 (d,  $J = 8.4\text{Hz}$ , 4H), 8.63 (d,  $J = 4.4\text{Hz}$ , 4H,  $\beta$ -pyrrolic H), 9.11 (d,  $J = 4.8\text{Hz}$ , 4H,  $\beta$ -pyrrolic H), 9.61 (s, 2H, CHO).

**3c:** 171.0 mg, 86% yield.  $^1\text{H}$  NMR (400 MHz,  $\text{CDCl}_3$ ,  $\delta$ ): 0.61–0.66 (m, 12H,  $\text{CH}_3$ ), 0.82–0.86 (t,  $J = 7.2\text{Hz}$  6H), 0.89–0.93 (t,  $J = 7.2\text{Hz}$  6H), 0.98–1.05 (m, 26H,  $\text{CH}_2$ ), 1.17–1.29 (m, 8H,  $\text{CH}_2$ ), 1.36–1.39 (m, 12H,  $\text{CH}_2$ ), 1.42–1.53 (m, 12H,  $\text{CH}_2$ ), 1.73–1.77 (m, 4H,  $\text{CH}_2$ ), 1.87–1.91 (m, 4H,  $\text{CH}_2$ ), 2.23–2.27 (m, 4H,  $\text{CH}_2$ ), 2.66–2.70 (m, 4H,  $\text{CH}_2$ ), 2.85–2.88 (m, 4H,  $\text{CH}_2$ ), 4.17–4.20 (m, 4H,  $\text{OCH}_2$ ), 4.27–4.31 (m, 4H,  $\text{OCH}_2$ ), 5.08–5.16 (m, 2H, CH), 7.37–7.45 (m, 4H, ArH), 9.56–9.58 (m, 2H,  $\beta$ -pyrrolic H), 9.63–9.66 (m, 2H,  $\beta$ -pyrrolic H), 9.81–9.88 (m, 4H,  $\beta$ -pyrrolic H), 10.44 (s, 2H, CHO).

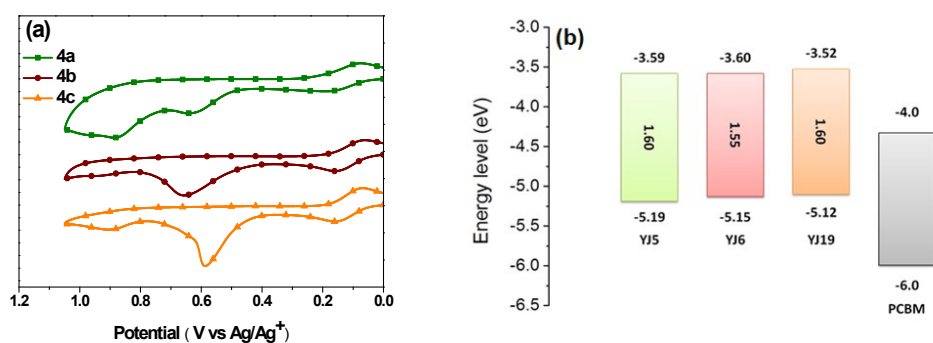


**Figure S1.** (a) Cyclic voltammograms of **4(a–c)** films in acetonitrile containing 0.1M  $\text{TBAPF}_6$  with a scan rate of  $50\text{ mV s}^{-1}$ , and (b) energy level diagram of **4(a–c)** and PCBM.

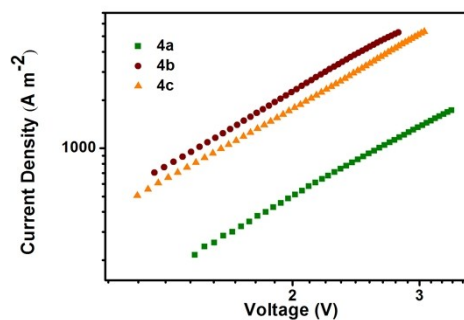


**Figure S2.** *J-V* characteristics of the hole-only devices in a configuration of ITO/PEDOT:PSS/active layer/MoO<sub>3</sub>/Al.

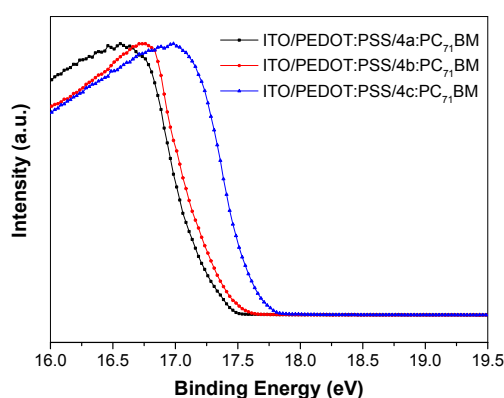


**Figure S3.** Ultraviolet photoelectron spectroscopy of ITO/PEDOT:PSS/4(a-c):PC<sub>71</sub>BM. Films of PEDOT:PSS/4a-c:PC<sub>71</sub>BM on ITO after annealing at 90 °C for 10 min.

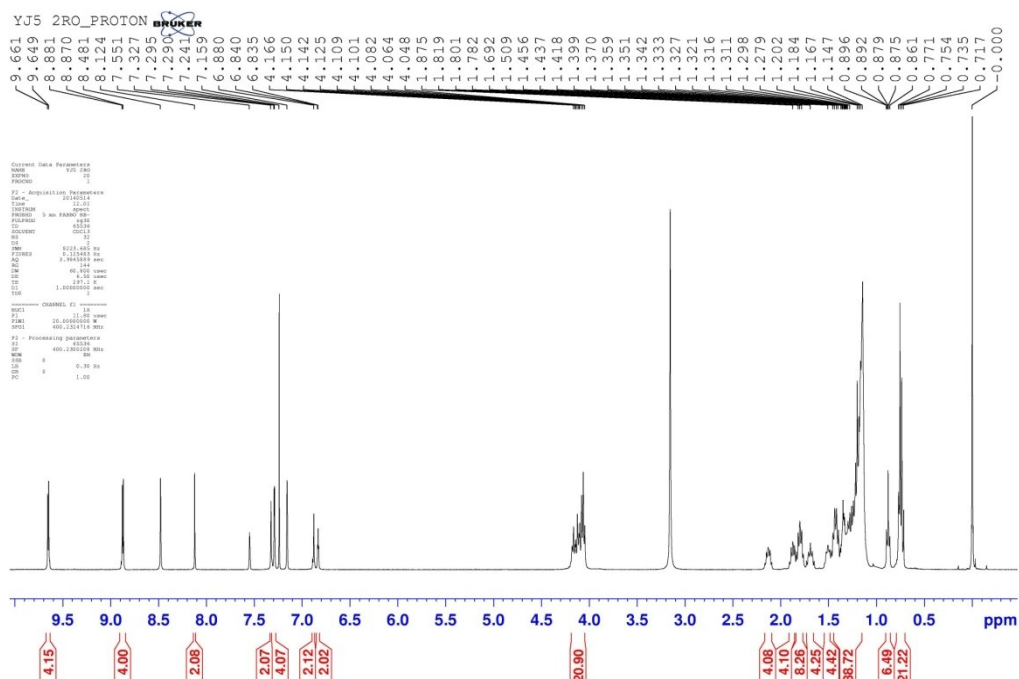


**Figure S4.** <sup>1</sup>H NMR spectrum of **4a**.

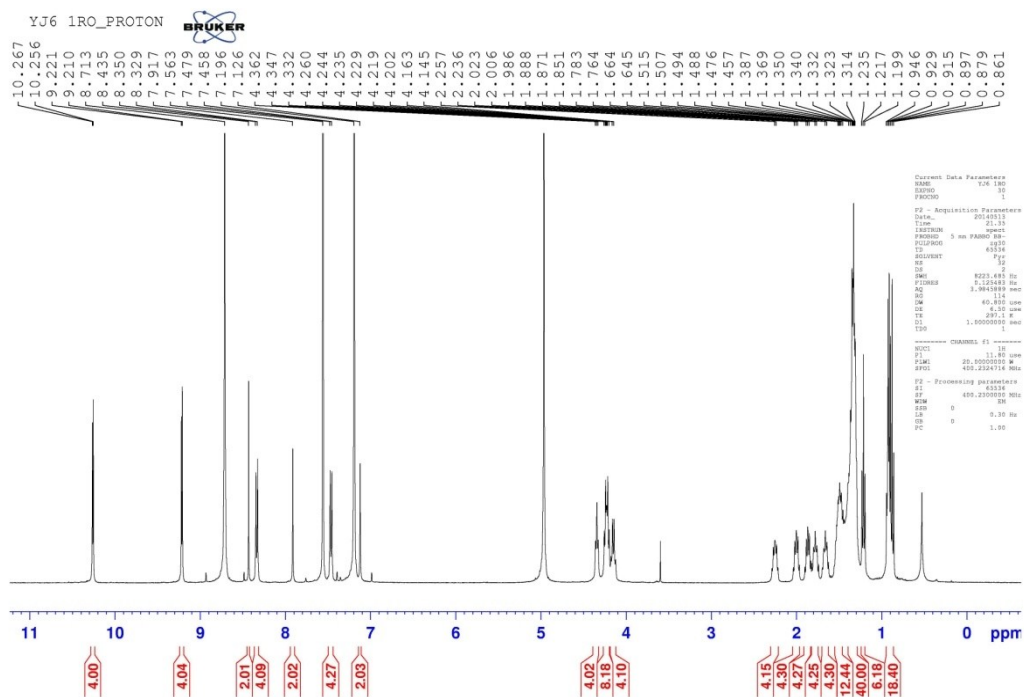


Figure S5.  $^1\text{H}$  NMR spectrum of **4b**.

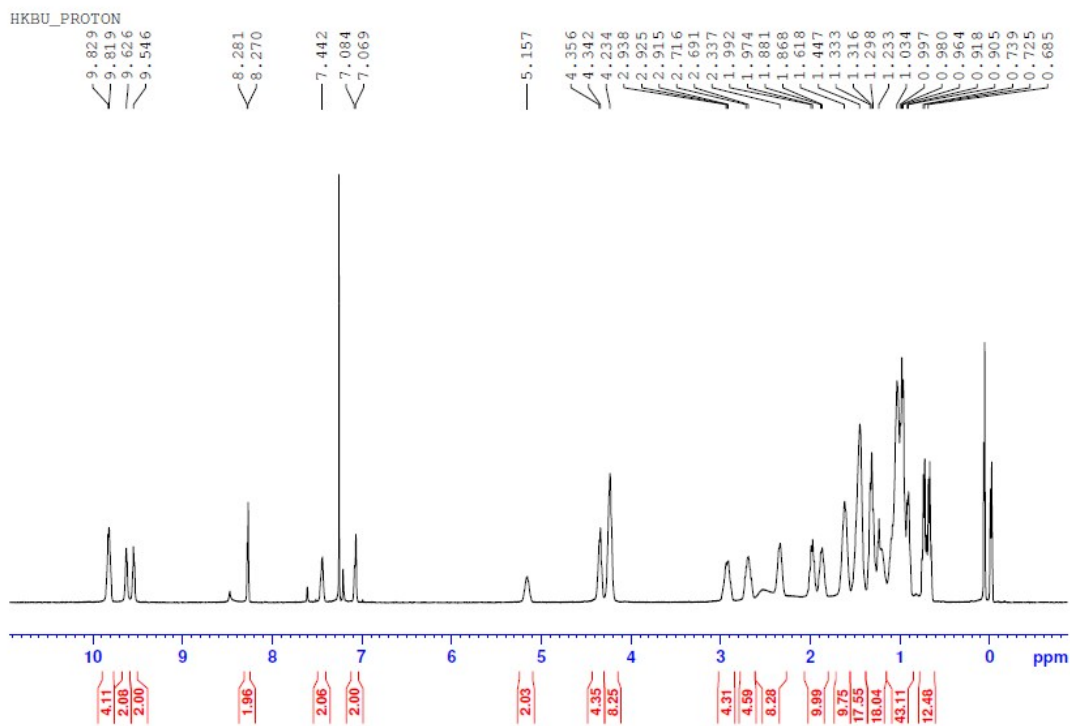


Figure S6.  $^1\text{H}$  NMR spectrum of **4c**.



HONG KONG BAPTIST UNIVERSITY, DEPARTMENT OF CHEMISTRY (MALDI-TOF)

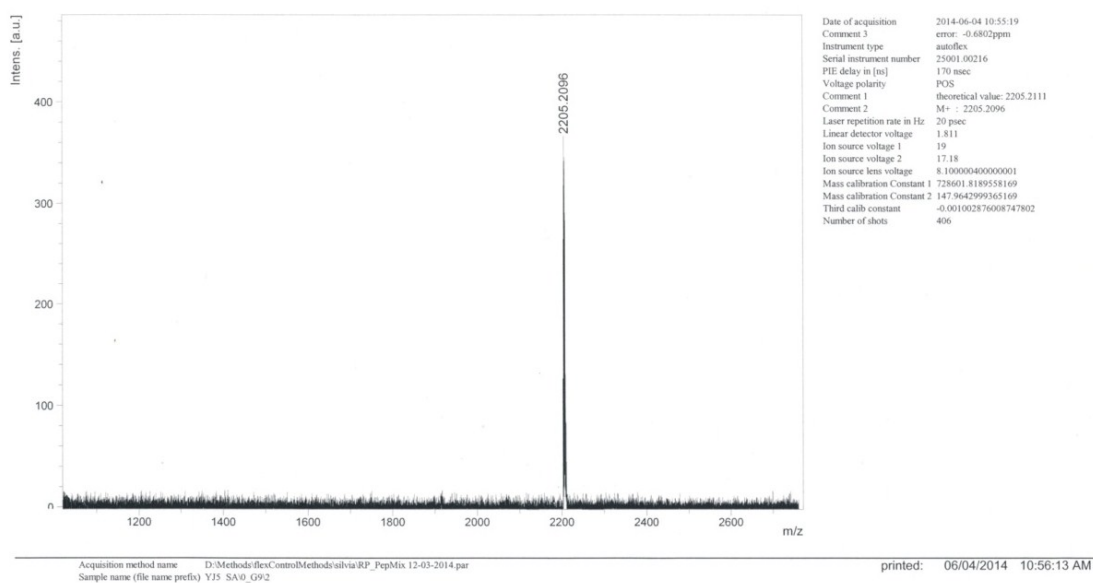


Figure S7. MALDI-TOF mass spectrum for 4a.

HONG KONG BAPTIST UNIVERSITY, DEPARTMENT OF CHEMISTRY (MALDI-TOF)

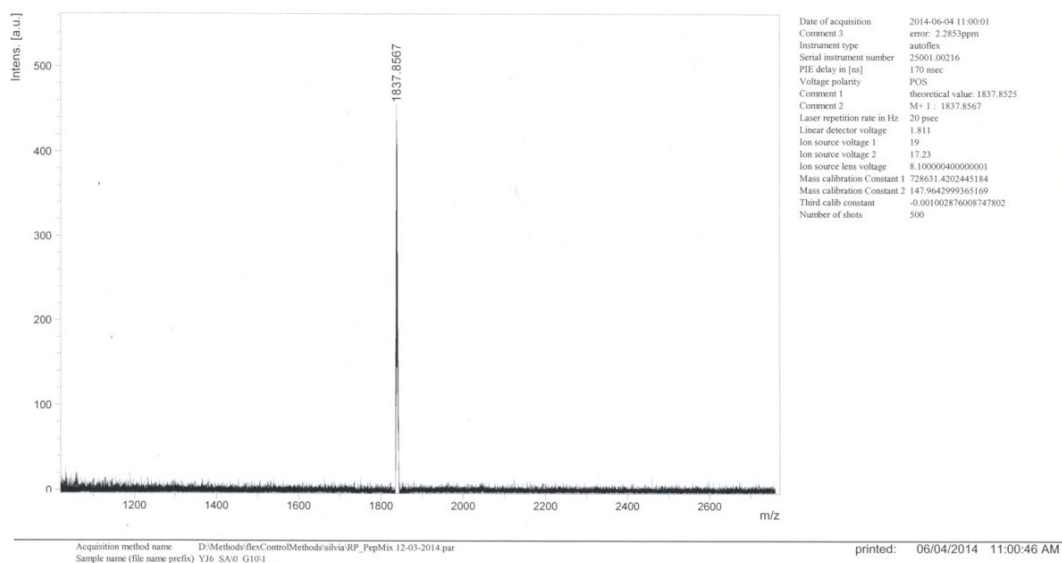


Figure S8. MALDI-TOF mass spectrum for 4b.

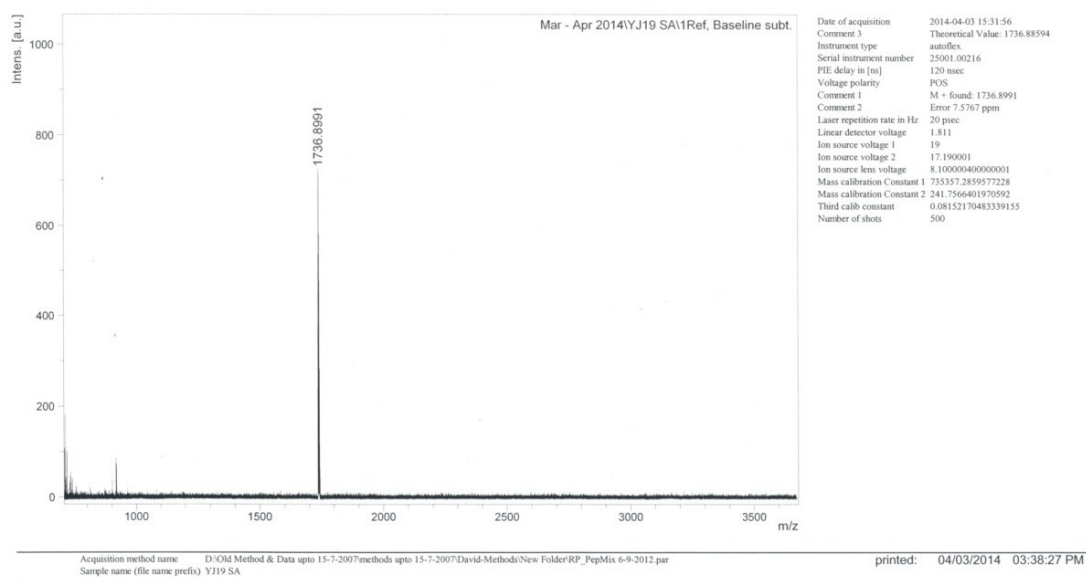


Figure S9. MALDI-TOF mass spectrum for 4c.